System, Report No. 5), Department of Computer Science, The Pennsylvania State University, University Park, PA.
DeMaine, P. A. D. (1980b) in *Automatic Systems for the Physical Sciences* (System Manual for the CRAMS System, Report No. 6), Department of Computer Science, The Pennsylvania State University, University Park, PA.
Dev, I. K., & Harvey, R. J. (1978) *J. Biol. Chem. 253*, 4245.
Fersht, A. (1977) *Enzyme Structure and Mechanism*, p 97, W. H. Freeman, San Francisco.
Kallen, R. G., & Jencks, W. P. (1966) *J. Biol. Chem. 241*, 5851.
Kisliuk, R. L., Gaumont, Y., Lafer, E., Baugh, C. M., & Montgomery, J. A. (1981) *Biochemistry 20*, 929.
MacKenzie, R. E., & Baugh, C. M. (1980) *Biochim. Biophys. Acta 611*, 187.
Mathews, C. K., & Huennekens, F. M. (1960) *J. Biol. Chem. 235*, 3304.
Matthews, R. G., & Baugh, C. M. (1980) *Biochemistry 19*, 2040.
Mueller, W. T., & Benkovic, S. J. (1981) *Biochemistry 20*, 337.
Paukert, J. L., D'Ari Straus, L., & Rabinowitz, J. C. (1976) *J. Biol. Chem. 251*, 5104.
Paukert, J. L., Williams, G. R., & Rabinowitz, J. C. (1977) *Biochem. Biophys. Res. Commun. 77*, 147.
Rabinowitz, J. C., & Pricer, W. E. (1962) *J. Biol. Chem. 237*, 2898.
Rowe, P. B. (1968) *Anal. Biochem. 22*, 166.
Schirch, L. (1978) *Arch. Biochem. Biophys. 189*, 283.
Segal, I. H. (1975) *Enzyme Kinetics*, pp 100–105, Wiley, New York.
Smith, G. K., Mueller, W. T., Wasserman, G. F., Taylor, W. D., & Benkovic, S. J. (1980) *Biochemistry 19*, 4313.
Smith, G. K., Benkovic, P. A., & Benkovic, S. J. (1981) *Biochemistry 20*, 4034.
Storer, A. C., & Cornish-Bowden, A. (1974) *Biochem. J. 141*, 205.
Tan, L. U. L., & MacKenzie, R. E. (1977) *Biochim. Biophys. Acta 485*, 52.
Tan, L. U. L., Drury, E. J., & MacKenzie, R. E. (1977) *J. Biol. Chem. 252*, 1117.
Uyeda, K., & Rabinowitz, J. C. (1967a) *J. Biol. Chem. 242*, 24.
Uyeda, K., & Rabinowitz, J. C. (1967b) *J. Biol. Chem. 242*, 4378.
Zamenhof, S. (1957) *Methods Enzymol. 3*, 696.

Reaction of Arsenite Ions with the Molybdenum Center of Milk Xanthine Oxidase†

Graham N. George and Robert C. Bray*

ABSTRACT: A study has been made of the reaction of arsenite ions with milk xanthine oxidase. In agreement with earlier work, the reaction was found to take place exclusively at the molybdenum site of the functional enzyme and is accompanied by loss of enzymic activity. The product of the reaction may be reduced and reoxidized without change of properties and can exist in Mo(VI), Mo(V), and Mo(IV) states. The Mo(VI) state of the arsenite complex is confirmed to have a characteristic absorption band at 380 nm, relative to the untreated enzyme, but this band is not present in the Mo(IV) state. Kinetic studies of the reaction of arsenite with the oxidized molybdenum center indicate a complex process in which initial reversible binding is followed by a slower irreversible process with $k = 0.020\ s^{-1}$ at pH 8.2 and 25 °C. The dithionite-reduced enzyme reacts much faster with arsenite than does the oxidized enzyme. The presence of competitive inhibitors or substrates slows the reaction with arsenite, both for the reduced and for the oxidized enzyme. The Mo(V) state of the arsenite complex gives a very complicated electron paramagnetic resonance (EPR) spectrum that has been successfully interpreted with the aid of computer simulations for spectra at 9 and 35 GHz. There is not only strong anisotropic hyperfine coupling but also strong quadrupole coupling of a single arsenic nucleus to molybdenum. Relevant parameters, including angular relationships, have been evaluated. Studies involving ^{2}H, ^{17}O, and ^{33}S substitution show no coupling to ^{1}H but weak coupling to ^{33}S and to ^{17}O. The nature of the reaction with arsenite and the structure of the arsenite complex are discussed. A structure of the form >Mo(=O)S—As= is proposed, in which the sulfur atom is the cyanide-labile sulfur originally present as Mo=S in the oxidized enzyme. In the arsenite complex, substrates and small inhibitor molecules have partial access to the active site, since they modify the EPR spectrum somewhat.

Studies of the reactions of various inhibitors with molybdenum centers in enzymes have been important in helping to elucidate their structures and mechanisms of action (Bray, 1980a). Arsenite ions have long been known to be inhibitory to xanthine oxidase [e.g., Barrey et al. (1928) and Peters & Sanadi (1961)] and to the other molybdenum-containing hydroxylases, xanthine dehydrogenase, and aldehyde oxidase (Coughlan et al., 1969). This inhibition is accompanied by changes in the absorption spectra of the enzymes with a substantial increase in absorption at 380 nm (Coughlan et al., 1969; Cleere & Coughlan, 1974). Johnson & Rajagopalan (1978) found that the molybdenum(V) EPR[1] spectrum of

† From the School of Chemistry and Molecular Sciences, University of Sussex, Falmer, Brighton BN1 9QJ, England. *Received August 13, 1982.* The work was supported by grants from the Medical Research Council, and G.N.G. received a studentship from the Science and Engineering Research Council.

[1] Abbreviations: EPR, electron paramagnetic resonance; EXAFS, X-ray absorption edge extended fine structure; Bicine, *N,N*-bis(2-hydroxyethyl)glycine.

0006-2960/83/0422-1013$01.50/0

arsenite-inactivated xanthine dehydrogenase was different from that of active enzyme, indicating that the arsenite is binding near to the molybdenum site in the enzyme. Coughlan et al. (1969) found that the reaction of all three molybdenum-containing hydroxylases with arsenite was reversible, though not readily so. For aldehyde oxidase reversal occurred rapidly (development of the inhibition also occurs rapidly), and for xanthine oxidase and dehydrogenase (whose reaction is slow), it occurred on extreme treatment only, such as heating at 50 °C for 2 h. These workers also found that prolonged exposure of the arsenite-inactivated enzymes to cyanide caused removal of the optical features associated with the arsenite complex and appearance of those associated with the desulfoenzyme. This indicated that the reaction of arsenite is closely associated with the cyanolysable sulfur, which studies by EXAFS (Bordas et al., 1980; Cramer et al., 1981) and EPR (Malthouse et al., 1981) have shown to be a terminal sulfur ligand of molybdenum.

The arsenite complex of xanthine oxidase is of interest for at least two reasons. First, its EPR spectrum is a complex one, and preliminary investigation (S. Gutteridge and R. C. Bray, unpublished results) had indicated that its powder line shape could not be simulated by using the simple programs of Lowe (1978), with hyperfine coupling from one ^{75}As nucleus. Possible explanations were as follows: (i) The complexity of the spectrum was due to two or more ^{75}As nuclei causing hyperfine splitting of the molybdenum(V) signal. (ii) That arsenite was reacting with the active center in more than one way, leading to the presence of more than one chemical species, yielding superimposed EPR spectra each showing coupling of ^{75}As to molybdenum(V). Or, finally, (iii) that quadrupole coupling to the ^{75}As nucleus was present. In this connection, Belford & Duan (1978) have shown that it is possible to estimate quadrupole coupling parameters from EPR powder line shapes. Demonstration of this in the arsenite complex of the enzyme would be of chemical interest as examples of quadrupole coupling from ligands to transition-metal complexes, even in nonbiological systems, are rare.

Second, the reaction is of interest in relation to the structure and action of molybdenum centers in enzymes. The kinetics of the inhibitory reaction have not been substantially investigated, and their study, together with evaluation of EPR parameters, could provide information on the structure of the arsenite complex and on the nature of the reaction, with possible mechanistic implications. We now report a detailed study of the reaction of xanthine oxidase with arsenite ions, including interpretation of the EPR spectrum, confirming the importance of quadrupole coupling.

Materials and Methods

General. Unless otherwise stated, all experiments were carried out at 25 °C in 50 mM sodium–Bicine buffer at pH 8.2. Milk xanthine oxidase was prepared by the salicylate denaturation procedure (Bray, 1982; Hart et al., 1970). The desulfo form was prepared by treatment of the enzyme with cyanide (Massey & Edmondson, 1970). ^{33}S-Enriched xanthine oxidase was prepared by reconstitution of the desulfo form with ^{33}S-enriched sodium sulfide (Malthouse & Bray, 1980; Malthouse et al., 1981). Water enriched with ^{17}O was obtained from Monsanto Research Corp. at an enrichment of 52.4 atom %, and xanthine oxidase samples exchanged with ^{17}O were prepared by using the method of Bray & Gutteridge (1982). ^{17}O-Substituted sodium arsenite was prepared by heating the salt with ^{17}O-labeled water in a sealed glass tube for 8 days at 130 °C [by analogy with the method for phosphate (Boyer & Bryan, 1967)] and then evaporating to dryness. Experiments in ^2H_2O were carried out as described by Gutteridge et al. (1978a). Xanthine oxidase concentrations are expressed as concentrations of functional active centers calculated from ϵ_{450} (per half-mol) = 36000 M^{-1} cm^{-1} and limiting activity/A_{450} of 190 (Bray, 1975). All absorbance measurements were made on a Unicam SP1800 spectrophotometer, and computer manipulation of suitably digitalized optical data was performed upon a PDP 11/10 computer.

Enzyme Assays. Xanthine oxidase activity at 25 °C was monitored by following the increase in absorbance at 295 nm caused by uric acid formation in a mixture containing 0.1 mM xanthine and in equilibrium with atmospheric oxygen (buffer as described above). The reaction was started by addition of xanthine oxidase to a final concentration of about 45 nM.

Inactivation of Oxidized Xanthine Oxidase with Arsenite. Arsenite (e.g., 0.2–1 mM final concentration) was added to xanthine oxidase (final concentration about 30 μM) and the reaction was monitored by following the absorbance at 380 nm. Alternatively, samples were removed from the mixture for assays at appropriate times (the dilution being such that the final concentration of arsenite in the assay would have been insufficient to affect activity). Under the above conditions, reaction (at pH 8.2 and 25 °C) was complete in about 60 min. Once prepared, the arsenite complex was stable to gel filtration or to concentration of the enzyme by ultrafiltration.

Inactivation of Reduced Enzyme with Arsenite. For reduced xanthine oxidase, inactivation was followed by monitoring loss of enzymic activity. The reaction was carried out anaerobically in glass vessels closed with rubber septa under an atmosphere of purified argon. The enzyme (final concentration about 30 μM) was first reduced with sodium dithionite (5 mM final concentration) for 30 min at 0 °C. The reaction was then started by anaerobic addition of sodium arsenite solution. Approximately every 20 s, samples were withdrawn through the rubber septum by use of a syringe and assayed as described above.

Preparation of Samples for EPR Spectroscopy. Concentrated enzyme samples in quartz tubes were suitably reduced, anaerobically under an atmosphere of purified argon. Generally, molybdenum(V) signals were developed by reducing arsenite-treated xanthine oxidase (0.3 mM) with sodium dithionite (2 mM final concentration) for 90 s and then freezing in liquid nitrogen. Rapid freezing was carried out according to Gutteridge et al. (1978a).

Experimental and Computer-Simulated EPR Spectra. EPR spectra were recorded on a Varian E9 spectrometer linked to a computer and visual display system (Bray et al., 1978). Samples were run at −150 °C, with a time constant of 0.3 s. For spectra at 9 GHz, 10-mW microwave power and a modulation amplitude of 0.16 mT were used, and for those at 35 GHz, 10-dB attentuation with a modulation amplitude of 0.5 mT was used. Computer simulation of EPR powder line shapes was performed upon the University of Sussex DEC VAX 11/780 computer by fitting spectra to the Hamiltonian for an $S = {}^1/_2$ system with one set of hyperfine coupling:

$$\mathcal{H} = \beta \mathbf{H}\cdot\mathbf{g}\cdot\mathbf{S} + h\mathbf{S}\cdot\mathbf{A}\cdot\mathbf{I} + h\mathbf{I}\cdot\mathbf{P}\cdot\mathbf{I} - \beta_n g_n \mathbf{H}\cdot\mathbf{I} \qquad (1)$$

This was done by using the program QPOW written by R. L. Belford and co-workers (Nilges, 1979; Belford & Nilges, 1979; Maurice, 1980). In eq 1, all symbols have their usual meaning (Abragam & Bleaney, 1970). In the program, the **g** and **A** tensors[2] are assumed symmetric, the nuclear **g** matrix is as-

[2] **g** and **A** should really be termed interaction matrices, as they are not always true tensors (Abragam & Bleaney, 1970). However, in accordance with usual practice, they will be referred to as tensors here.

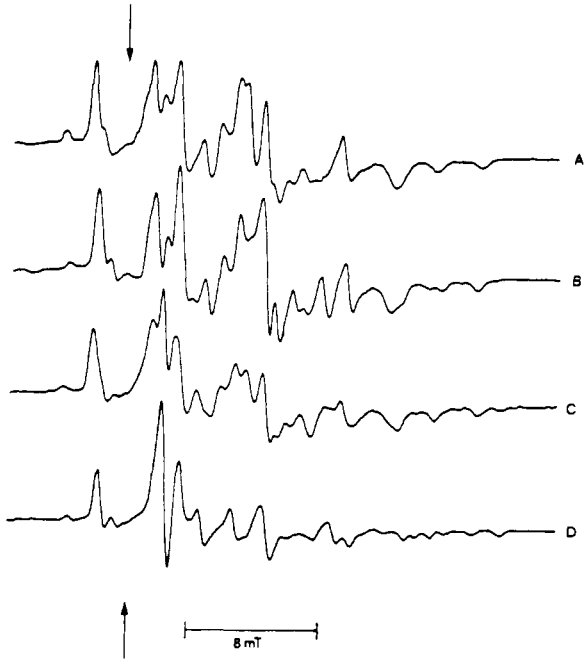

FIGURE 1: Effects of various substances upon the Arsenite Mo(V) EPR signal from xanthine oxidase. In this experiment (and in those of Figures 6–8) arsenite-treated xanthine oxidase from which excess arsenite had been removed (by gel filtration on a Sephadex G-25 column) was used and was reduced with sodium dithionite, as described under Materials and Methods. The effects of addition (prior to reduction of the enzyme) of various substances on the form of the Arsenite signal is illustrated. Spectrum A shows the signal with no additions and spectrum B is in the presence of 1 mM xanthine. [The addition of uric acid, purine, or allopurinol (all 1 mM) gave spectra indistinguishable from that shown in (B), with slight but characteristic differences from the control, (A).] (C) shows the signal developed in the presence of 5 mM benzoate and (D) in the presence of 1 mM salicylate, and they illustrate that these compounds cause larger changes in the form of the signal.

sumed isotropic with a value of 0.959, and the nuclear quadrupole coupling tensor is assumed symmetric and traceless.

Results and Discussion

Molybdenum(V) EPR Spectra from Reduced States of the Complex of Xanthine Oxidase with Arsenite. Figure 1A shows the molybdenum(V) EPR spectrum that we obtained on addition of dithionite to arsenite-treated xanthine oxidase. The line shape is a particularly complex one but was fully reproducible. We shall refer to the signal as the Arsenite signal. Evidence that it corresponds to a single chemical species was obtained from simulations of the spectrum at both 9 and 35 GHz and will be considered below. The Arsenite signal could be generated either by treating the enzyme with arsenite and then reducing with dithionite or, alternatively, by reversing the procedure and first reducing with dithionite and then adding arsenite. As is discussed below, activity loss and changes in the near-ultraviolet absorption spectrum accompanied the reaction of the enzyme with arsenite. The desulfoenzyme was not affected by arsenite, e.g., under the conditions used for generating the signal of Figure 1A.

Johnson & Rajagopalan (1978) reported that arsenite-inactivated xanthine dehydrogenase gave molybdenum(V) signals that showed substantial differences from those from active enzyme. They attributed these differences to hyperfine interaction with one or more ^{75}As nuclei. However, the signals that these workers presented were extremely badly resolved and largely obscured by the signal from flavin semiquinone, and no detailed interpretation was attempted. These workers also reported that purines and related substances changed the form of their molybdenum(V) signals, indicating that substrate binding could still occur in the arsenite complex. Figure 1B–D shows the effects of various substances upon the Arsenite signal. For purine, xanthine (Figure 1B), uric acid, or allopurinol, the spectra were indistinguishable from one another and only slightly different from the control with no additions (Figure 1A). However, the competitive inhibitors benzoate (Figure 1C) and salicylate (Figure 1D) caused quite large changes in the Arsenite signal. The significance of the binding of these substances to the arsenite complex will be considered later.

Reduction and Reoxidation of the Arsenite Complex. Treatment of the oxidized enzyme with arsenite did not give rise to any EPR signals. However, if such treatment was followed by reduction, under various conditions with dithionite, the Arsenite molybdenum(V) signal was observed. Under appropriate conditions of reduction this signal was accompanied by normal FADH· and iron–sulfur signals (Bray, 1975). If the treatment with arsenite had been taken to completion (see below), then under no conditions of reaction with dithionite was the Rapid molybdenum(V) signal, which is characteristic of the normal active enzyme, observed. However, under appropriate conditions of reduction the Slow signal from the desulfoenzyme was observed in its normal form. Thus, in agreement with Coughlan et al. (1969), we conclude that arsenite reacts exclusively at the molybdenum center of functional xanthine oxidase molecules.

In rapid freezing experiments, we found that the Arsenite signal was maximally developed in enzyme pretreated with arsenite after 90-s exposure to 2 mM dithionite. After this time, the signal graudally decreased in intensity, until after about 5 h no molybdenum(V) Arsenite signal could be seen. The integrated intensity of the Arsenite signal corresponds, at maximal development, to about 30% of the molybdenum of the functional enzyme. These results indicate that the molybdenum is first reduced from Mo(VI) to Mo(V), and then further reduced to Mo(IV). Under no conditions we tried did the substrates xanthine, purine, glycoaldehyde, or acetaldehyde reduce the oxidized arsenite complex. On the other hand, on exposure to air, the dithionite-reduced arsenite-treated enzyme was rapidly reoxidized, as indicated by all EPR signals disappearing. Further additions of dithionite caused redevelopment of EPR signals, as described above.

Reaction of oxidized xanthine oxidase with arsenite was accompanied by development of an absorption band centered at 380 nm, with a molar extinction of 6200 M^{-1} cm^{-1}/Mo, as reported by earlier workers (Coughlan et al., 1969). This is illustrated in Figure 2a. On reduction of the arsenite complex, no optical difference spectrum was detected relative to reduced untreated enzyme (Figure 2b). (The same was true when the above procedure was reversed and the enzyme was first reduced and then reacted with arsenite.) However, on reoxidation a spectrum very similar to that of the oxidized arsenite complex was seen, Figure 2c.

The above results show that the arsenite complex is stable to oxidation and reduction of the molybdenum site, which, as in active enzyme, can be Mo(VI), Mo(V), or Mo(IV), and that the flavin and iron–sulfur centers are unaffected by arsenite binding. We have not attempted to measure the oxidation–reduction potential of molybdenum in the arsenite complex. On the other hand, our data on maximum conversion to Mo(V) and on the kinetics of reduction with dithionite are both indicative of similarities of the arsenite complex to the normal active enzyme [cf. Bray et al. (1975) and Cammack et al. (1976)].

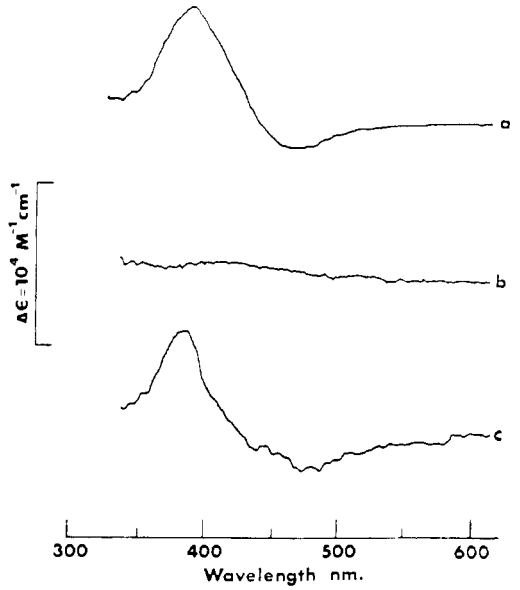

FIGURE 2: Optical difference spectra of oxidized and reduced arsenite-treated xanthine oxidase. (a) Optical difference spectrum, obtained as oxidized arsenite-treated enzyme minus oxidized enzyme. The spectrum in characterized by a large "positive" peak at 380 nm and a smaller "negative" peak at 460 nm. (b) Corresponding difference spectrum for the reduced xanthine oxidase–arsenite complex (reduced arsenite complex minus similarly reduced enzyme); (c) effect of reoxidizing the sample from (b) by bubbling both control and experimental samples with oxygen gas for 1 min. The difference spectrum has been restored to close to that in (a).

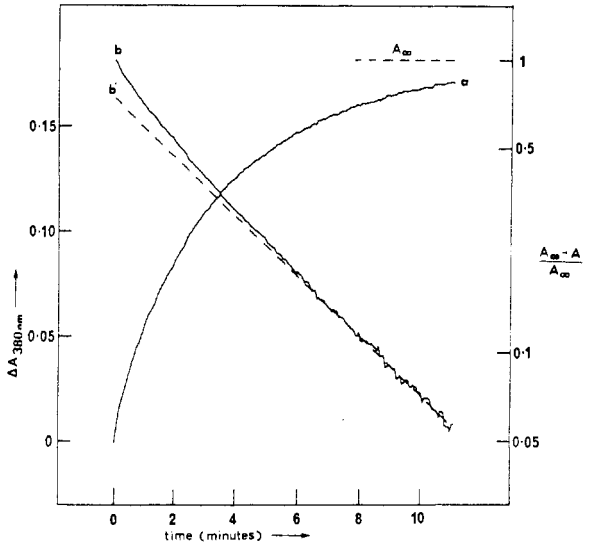

FIGURE 3: Kinetics of change in A_{380} during reaction of oxidized xanthine oxidase with 2 mM arsenite. (a) Absorbance change at A_{380} as a function of time, when using 2 mM arsenite and 30 μM oxidized xanthine oxidase. (b) Semilogarithmic plot, from the same experiment, of absorbance change with time, which indicates that the reaction is essentially first order. First-order rate constants (as employed in the experiments of Figure 4) were measured from the slopes of the linear parts of semilogarithmic plots of this type.

Kinetics of Reaction between Oxidized Xanthine Oxidase and Arsenite. A study of the reaction between oxidized xanthine oxidase and arsenite was carried out, following the reaction either by measurement of the absorbance at 380 nm or by assays for enzyme activity. Figure 3 shows that the reaction is essentially first order; however, a distinct fast phase was observed in the initial stages of the reaction. The possible nature of this fast phase will be discussed later. Figure 4 shows a plot of the inverse of pseudo-first-order rate constants (obtained from the final linear part of semilogarithmic plots such as that in Figure 3) vs. the inverse of the arsenite concentrations. The linearity of such a plot is typical of a reaction sequence of the form:

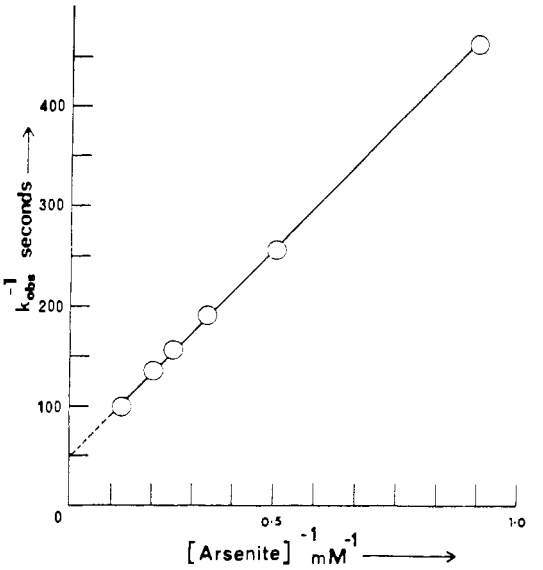

FIGURE 4: Reaction of oxidized xanthine oxidase with arsenite: double-reciprocal plot for rate constant and arsenite concentration. Plot of $1/k_{obsd}$ for the linear part of semilogarithmic plots (derived from absorbance measurements) such as that shown in Figure 3 vs. the reciprocal of arsenite concentration. The parameters derived from this plot are $k_{-1}/k_1 = 8.4$ mM and $k_2 = 0.020\ s^{-1}$, where k_1, k_{-1}, and k_2 are as described in eq 3.

$$E + A \underset{k_{-1}}{\overset{k_1}{\rightleftharpoons}} EA \xrightarrow{k_2} EA' \qquad (2)$$

(Strickland et al., 1975), where E represents xanthine oxidase, A represents arsenite, EA and EA′ represent forms with arsenite bound to enzyme, and k_1 and k_{-1} both represent reactions fast relative to that governed by k_2. The apparent rate constant k_{obsd} is then given by

$$k_{obsd} = k_2[A]/([A] + k_{-1}/k_1) \qquad (3)$$

A plot of $1/k_{obsd}$ vs. $1/[A]$ therefore gives a straight line of slope $k_{-1}/(k_2k_1)$ and intercept on the k_{obsd} axis of $1/k_2$. The data in Figure 4 thus gives values for k_2 of 0.020 s^{-1} and for k_{-1}/k_1 of 8.4 mM.

The fast phase in the reaction (Figure 3) was found also in measurements of loss of enzyme activity with time (not illustrated). The presence of this fast phase further illustrates the complexity of the reaction. It might be explained, e.g., by two parallel reactions, one proceeding faster than the other; however, this phenomenon was not investigated further.

Addition of a variety of substances to the reaction mixture was found to reduce significantly the rate of reaction of the enzyme with arsenite. These included salicylate, uric acid, and benzoate, all of which are known competitive inhibitors of xanthine oxidase activity.

Kinetics of Reaction between Reduced Xanthine Oxidase and Arsenite. The reaction of dithionite-reduced enzyme with arsenite was monitored by following loss of enzyme activity with time (Figure 5). The reaction is pseudo first order and very much faster than the reaction with oxidized enzyme. Because of the difficulty of accurately determining rate constants at high (i.e., >1 mM) arsenite concentrations, it was not possible to test whether kinetics similar to those for oxidized enzyme were followed (cf. eq 3). However, some comparison between the oxidzed and reduced forms may be made under conditions of low arsenite concentration since the limit

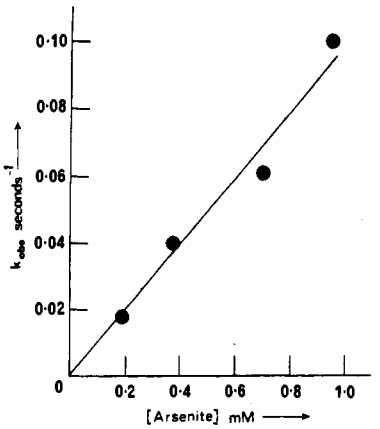

FIGURE 5: Kinetics of reaction of reduced xanthine oxidase with arsenite. The pseudo-first-order rate constant for the reaction of reduced enzyme and arsenite, derived from activity measurements, is plotted against arsenite concentration. Due to the high rate of reaction, it could not be determined whether the plot becomes nonlinear at high arsenite concentrations, as does that for the reaction with oxidized enzyme. The solid line was calculated from a linear regression constrained to go through the origin, which gave a second-order rate constant for the reaction of 98 M^{-1} s^{-1}.

of eq 3, as [A] tends to 0, is $k_2k_1[A]/k_{-1}$; i.e., the reaction is predicted to behave as a simple second-order reaction. On this basis, an apparent second-order rate constant of 2.38 M^{-1} s^{-1} calculated for oxidized enzyme may be compared with the much higher second-order rate constant of 98 M^{-1} s^{-1} deduced for reduced enzyme from Figure 5.

Our results conflict with those reported in a preliminary communication by Hille et al. (1982), who reported that reduced xanthine oxidase did not react with arsenite (reducing agent not specified). This could be explained if these workers used high concentrations of a substrate to reduce the enzyme. Thus, it was found in the present work that the presence of 0.1 mM xanthine decreased the pseudo-first-order rate constant for reaction of the enzyme with 0.67 mM arsenite in the presence of dithionite from 0.061 to 0.0076 s^{-1}. Our overall conclusion from these results is thus that arsenite reacts very much more readily with reduced than with oxidized xanthine oxidase.

Interpretation of the EPR Spectrum of the Arsenite Complex. Arsenic occurs only as ^{75}As, which has $I = {}^3/_2$. Thus a simple rhombic species showing coupling from a single arsenic atom to molybdenum would in the absence of such features as overshoot lines show four-line patterns in the g_1, g_2, and g_3 features. However, Figure 1A shows many more than the 12 turning points expected on such a simple basis. Furthermore, all "additional" features seem too large to be accounted for by the 25% of the naturally abundant isotopes ^{95}Mo and ^{97}Mo, which have $I = {}^5/_2$. Nevertheless, we found that all the features of the spectrum of Figure 1A were fully reproducible when, for example, pH (in the range 6–10), reaction time, or arsenite concentration (in the range 0.5–500 mM) was varied. This strongly suggests that only a single species is involved.

It seemed probable that quadrupole coupling from ^{75}As could be responsible for the complex form of the signal. This is a phenomenon that, at certain orientations of external magnetic field causes M_I no longer to be a good quantum number, resulting in shifts of field for the main ($\Delta M_I = 0$) transitions together with an increase in the intensity of the so-called "forbidden" transitions ($\Delta M_I = \pm 1$, $\Delta M_I = \pm 2$, and $\Delta M_I = \pm 3$ for $I = {}^3/_2$), thus resulting in a far more complex spectrum than would be seen if quadrupole coupling were absent.

Table I: EPR Parameters for the Mo(V) Arsenite Signal[a]

axis	g values	A (MHz)	P (MHz)	half line widths (MHz) 9 GHz	35 GHz
1	1.9258	−90	−10	12	25
2	1.9732	−40	27	6	16
3	1.9718	128	−17	6	16
av	1.9569	−1		8	19

[a] Values given were obtained as described in the text and were used for the simulations of Figures 6B and 7B. Euler angles for **A** and **P**: $\alpha = 15.0°$, $\beta = 0°$, and $\gamma = 0°$. 1 mT = 27.4 MHz for $g = 1.9569$.

Quadrupole coupling, as detected by EPR, is well-known for many transition metal complexes (White & Belford, 1976; Belford & Duan, 1978) and in other systems, including ^{75}As radicals (Geoffroy & Llinares, 1980). However, few examples of quadrupole coupling of ligand nuclei in transition metal complexes are known (Kubo & Nakamura, 1966) even outside the biological field and even fewer have been detected by EPR [see, for example, Nilges et al. (1977)].

Simulation of the Arsenite spectrum appeared to us to be obligatory both in order to verify the hypothesis that quadrupole coupling was indeed responsible for its complexity and in order to evaluate the parameters. Achievement of both of these objectives was made feasible by the availability of computer programs developed by R. L. Belford (see Materials and Methods). However, general verification of the hypothesis would of course be expected to be much simpler than quantitative evaluation of the parameters. If the spectrum both at 9 and at 35 GHz could be simulated by using a single set of parameters, this would greatly increase confidence in the rigor of the interpretation and in the correctness of the parameters. We therefore recorded the Arsenite signal at 35 GHz (Figure 7A). If nothing is known about the values of the various parameters, then there are clearly an extremely large number of possibilites to be investigated in simulations. Therefore, the following approach was used: (i) The hyperfine tensor **A** and the quadrupole tensor **P** were held collinear; this assumption is reasonable as it has been found to apply to other systems (Nilges & Belford, 1979; Nilges et al., 1977). (ii) The spectrum was first simulated with no quadrupole interaction, and this was only introduced when it became clear that no good fit could be obtained in its absence. (iii) More importance was attached to the appearance of the 9-GHz spectrum than to that at 35 GHz. The former has many more features, whose position is sensitive to small changes in the parameters, than does the latter.

The final best fit from about 100 simulation attempts is shown in Figures 6 and 7. If the various contributions (not illustrated) to the overall line shape are examined, it becomes apparent that the forbidden $\Delta M_I = \pm 2$ transitions provide some of the features of largest amplitude. The fit to the experimental data is not perfect, especially in the 35-GHz spectrum, and could no doubt be improved with still further effort. Minor deviations may be because of noncollinearity of **P** and **A** (but note the quality of the fit of the high-field region in this simulation). However, the parameters used (Table I) must be at least approximately correct. The signs of the hyperfine and the quadrupole coupling are only determined relative to one another, and if reversed, an equivalent simulation would result. However, the absolute signs are easy to deduce if we assume that electrons are withdrawn from the arsenic as a result of bonding. This would make the largest principal axis of **P** positive, resulting in the values given in

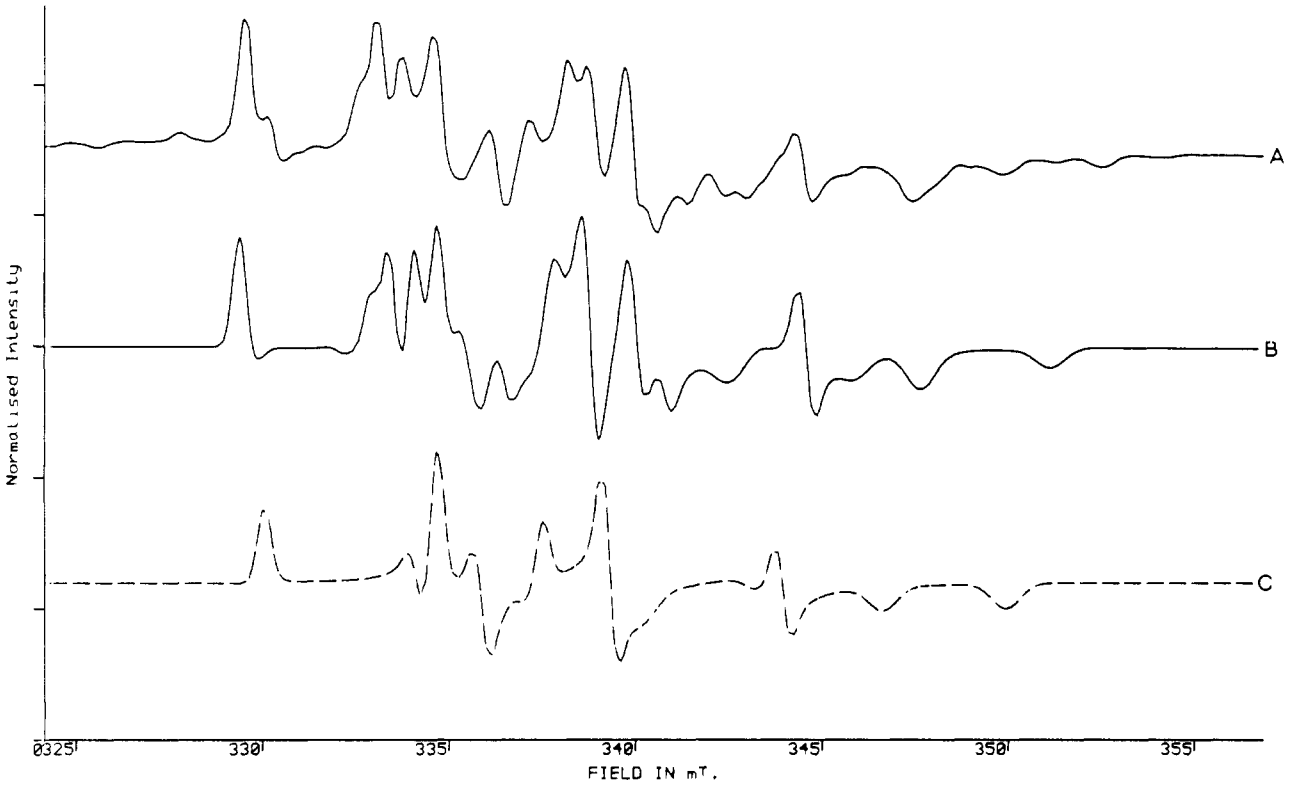

FIGURE 6: Simulation of the Arsenite signal at 9 GHz. The best computer simulation of the experimental spectrum (A) is shown in (B) and was obtained as described under Materials and Methods by using the parameters given in Table I. The fit is seen to be a fairly good one in most regions of the spectrum. (C) Effect of excluding quadrupole coupling parameters, all other parameters remaining the same. The fit of (B) to (A) is obviously markedly better than that of (C) to (A). The field scale corresponds to a microwave frequency of 9.301 GHz, and the experimental spectrum was generated as for Figure 1A.

Table I. The signs of the two smallest principal values of **A** (A_1 and A_2) should be considered arbitrary as changing them does not affect the simulation greatly.

Several points are worth noting about the values of the parameters. (i) The line widths are more anisotropic than for any other Mo(V) signals found in molybdoenzymes (Bray, 1980b). Since both 9- and 35-GHz spectra show anisotropic line widths, this is not due to a second weakly interacting ^{75}As nucleus. Anisotropy must be due to the hyperfine or quadrupole coupling somehow providing an extra, orientation-dependant, method of relaxation. (ii) The ^{75}As hyperfine interaction is highly anisotropic. (iii) There is also strong quadrupole coupling, the magnitude of this being comparable to that of the hyperfine interaction. Few systems are known where this is found to be the case. Structural implications of these findings will be discussed below.

Isotopic Substitution Studies. Studies involving substitution with various stable isotopes have been important in establishing the structures of different Mo(V) EPR signal-giving species for molybdenum-containing enzymes (Bray, 1980a; Malthouse et al., 1981; Gutteridge & Bray, 1980). We therefore carried out analogous studies on the Arsenite signal. The Arsenite signal prepared in ^2H_2O solution was not different from that prepared in ^1H_2O, showing that no hyperfine coupling to exchangeable protons is present. Figure 8 shows the effect of substitution of the cyanolysable sulfur by ^{33}S (Malthouse et al., 1981) or of exchanging the enzyme into ^{17}O-labeled water. It was found that ^{33}S gave only slight broadening, particularly of the central features of the signal (Figure 8B). This probably indicates a nearly isotropic hyperfine interaction of 2 MHz or rather less. ^{17}O-Substitution, on the other hand, gave apparently larger and more obviously anisotropic broadening (Figure 8C). The anisotropy is indicated by the peak at lowest field appearing relatively sharp, as do the peaks associated with turning points ascribed to the g_2 principal axis. On the other hand, most other features are considerably broadened, indicating that larger hyperfine coupling is associated with them. Preliminary simulations (not illustrated) of the ^{17}O Arsenite signal, based on coupling of Mo to a single ^{17}O as well as to ^{75}As, did not readily duplicate the line shape in Figure 8C. This probably indicates noncollinearity of **g** and **A** (^{17}O). Development of the Arsenite signal with ^{17}O-substituted arsenite gave a signal (not illustrated) that was not different from the control employing ordinary arsenite in ordinary water. This indicates that the remaining oxygens on arsenite are not involved in bonding to the molybdenum.

Hanson et al. (1981) have synthesized a MoO^{3+} compound, $MoO(SPh)^{4-}$, with ^{17}O-substituted terminal oxygen. They found the hyperfine coupling from this oxygen to be small and could measure only the isotropic (solution) coupling constant of 6.3 MHz. This low value was ascribed to this oxygen being in an axial type of position, rather than in an equatorial position, while the ground state 4d orbital is probably of the d_{xy} in-plane type. On the other hand, several Mo(V) signals from ^{17}O-substituted xanthine oxidase are known where the splitting is much larger [see, e.g., Gutteridge & Bray (1980) and Bray & Gutteridge (1982)]. In these, the oxygen is thought to be in an equatorial type of position. The weak hyperfine interaction from ^{17}O in the Arsenite signal suggests that the oxygen is an axial-type ligand, and the anisotropy argues for a large p-orbital contribution in the bonding, probably indicating a terminal oxygen. This conclusion is taken into account in Chart I.

Nature of the Reaction of the Enzyme with Arsenite and Structure of the Signal-Giving Species. The kinetic results and the parameters derived from interpretation of the EPR spectrum are both important in attempting to deduce the nature of the reaction between arsenite and the molybdenum

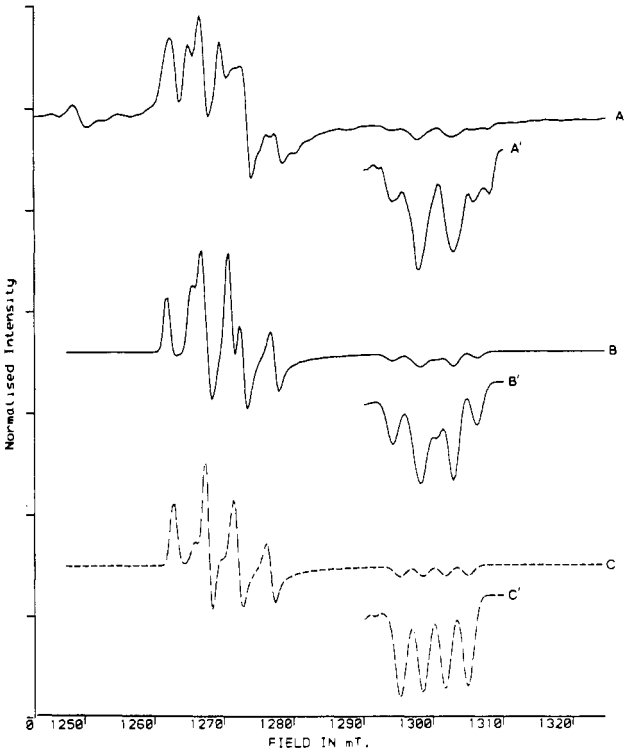

FIGURE 7: Simulation of the Arsenite signal at 35 GHz. (A) Arsenite signal at 35 GHz (generated as for Figure 1A) and (A′) high-field region of (A) vertically expanded 6-fold. (B) is the simulation of (A) obtained by using the parameters in Table I and (C) shows the effect of omitting quadrupole coupling parameters from the simulation. The fit of (B) is rather less good than the corresponding simulation at 9 GHz. However, the fit of the high-field region (A′) could only be reproduced (B′) when large quadrupole coupling was included, and (C′) shows the effect on this region of excluding quadrupole coupling from the simulation. The field scale corresponds to a microwave frequency of 35.05 GHz.

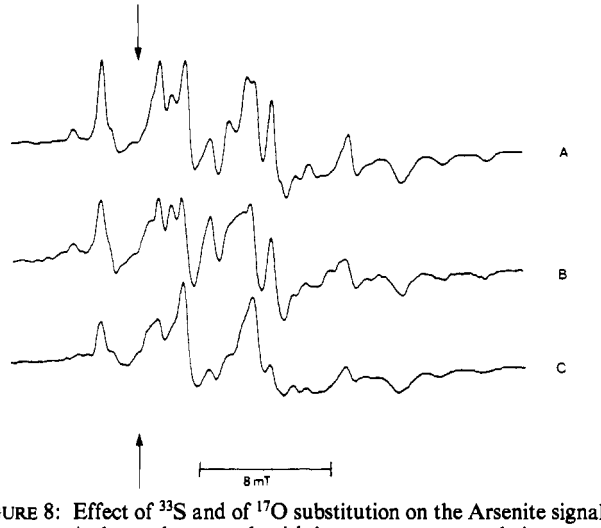

FIGURE 8: Effect of ^{33}S and of ^{17}O substitution on the Arsenite signal. Spectrum A shows the control, with isotopes present at their natural abundance; (B) is the spectrum for 100% ^{33}S obtained by difference procedures from 52% ^{33}S, as described by Malthouse et al. (1981). Spectrum C is the spectrum for 100% ^{17}O, assuming one oxygen nucleus coupled, and determined by difference procedures from 54% ^{17}O by using the methods of Bray & Gutteridge (1982). The coupling to ^{33}S is seen only as a slight broadening of the line shape, whereas ^{17}O causes larger, and apparently more anisotropic, hyperfine coupling features.

center of xanthine oxidase and the structure of the product. A number of molybdenum(V) compounds with ^{75}As ligand hyperfine coupling are known. These include the complexes of Marov et al. (1967), $[MoO(H_2AsO_4)_nCl_{(4-n)}]^-$, where n = 1–4, which show an isotropic (solution) coupling of the metal to ^{75}As of about 36 MHz. These workers also found that the isotropic g value decreased markedly with increasing number of arsenic nuclei coupled. The Arsenite signal has the lowest g values (Table I) of any Mo(V) signal from xanthine oxidase (Bray, 1980b). This may be due to spin–orbit coupling involving the arsenic. Other d^1 transition metal complexes showing coupling to ^{75}As nuclei are vanadyl complexes with dimethyldithioarsenate (Day & McClung, 1976; Baratova et al., 1982). In these complexes dimethyldithioarsenate acts as a bidentate ligand, forming four-membered rings containing two bridging sulfur atoms between the arsenic and vanadium atoms. These complexes give strong transannular hyperfine coupling of arsenic to molybdenum of about 120 MHz, which, typically in such bridged structures, is notably isotropic. Day & McClung (1976) found that the addition of pyridine (which ligated the vanadium) disrupted the cyclic structure so that the arsenic was then joined by only one sulfur and that this removed the large coupling to ^{75}As.

Chart I: Proposed Structure of the Arsenite Mo(V) Signal-Giving Species[a]

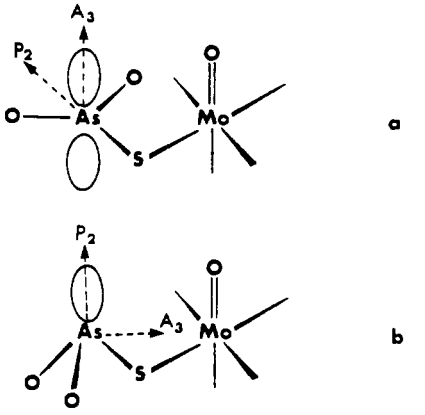

[a] The arsenite ion is shown having had one of its oxygen atoms replaced by the terminal sulfur of the oxidized molybdenum center, so that this sulfur bridges between As and Mo. The position of As is shown relative to an octahedral arrangement around Mo, which bears a terminal oxygen ligand, and with the directions of the arsenic hyperfine and quadrupole coupling axes indicated. Alternative a shows a planar arrangement of atoms around As, whereas alternative b shows a tetrahedral arrangement.

The bearing of these data upon possible structures for the Arsenite signal-giving species will now be considered. First, a cyclic type of structure with transannular coupling, such as the vanadyl complex discussed above, may be excluded from the large anisotropy of the ^{75}As ligand hyperfine coupling (Table I). The cyanide-labile terminal sulfur is essential for the reaction of arsenite with xanthine oxidase. As the high affinity of arsenite for thiols is well-known, it seems probable that the arsenite is reacting, in the reduced enzyme, with a molybdenum-bound thiol (Gutteridge et al., 1978b; Bray & Gutteridge, 1982; Cramer et al., 1981) and in the oxidized enzyme with the molybdenum-bound terminal sulfur (Bordas et al., 1980; Cramer et al., 1981). The precise chemistry of reaction between arsenite and terminal sulfur is, however, uncertain. In keeping with this, the kinetics we observed for reaction of the oxidized enzyme were complex. On the other hand, for reduced enzyme the observed much greater affinity for arsenite seems fully consistent with reaction with a thiol.

Arsenite has no effect upon desulfo xanthine oxidase, and it therefore seems unlikely that it reacts with more than one group in the molybdenum site of the active enzyme (potentially arsenite can react with three thiols). We therefore propose

a structure for the Arsenite signal-giving species, as shown in Chart I. The fact that the hyperfine coupling from ^{33}S is so small is not inconsistent with this scheme, since, in d^1 systems, the ligands adjacent to the metal tend to be weakly coupled as they lie in the nodes of the ground-state d orbital (usually of the in-plane d_{xy} type, for octahedral symmetry). The arsenic, on the other hand, could be held into a region of higher electron density by a bent Mo–S–As bond. This type of explanation is obviously not rigorous. However, it does hold for many d^1 systems where ligand hyperfine coupling is observed. It might be objected that the noncyclic vanadyl complexes of Day & McClung (1976), discussed above, with structures of this type, have very small ^{75}As hyperfine coupling and that this is inconsistent with the interpretation of Chart I. However, the arrangement in these structures could be affected by steric effects from the pyridine ligand, causing the V–S–As bond to become more nearly linear. Probably more significantly, the complexes of Marov et al. (1967) mentioned above have large hyperfine coupling to ^{75}As, and in these the arrangement is Mo–O–As, which is presumably analogous to our proposed Mo–S–As structure.

Evaluation (Table I) of the quadrupole coupling parameters, including angular information, permits further insights into the structure of the arsenite complex. The quadrupole coupling tensor **P** has its largest principal axis perpendicular to the largest principal axis of **A**. Two possibilities arise (Chart I). If the hyperfine coupling arose mainly from delocalization onto a p orbital (Chart Ia), then this would indicate that there is a large amount of asymmetry in the plane perpendicular to the axis of this p orbital. On the other hand, arsenic(III) is normally found, in its oxy anions, as a tetrahedral species. If this were the case, then the largest principal axis of **P** would be expected to point to the corner of the tetrahedral arrangement where there is no atom (Chart 1b). In this case, the observation that the largest axis of **P** is perpendicular to the largest axis of **A** is puzzling, since, if delocalization on to the arsenic was the principal cause of hyperfine coupling, then these axes should coincide. In this instance we would conclude that the hyperfine interaction must arise mostly from direct dipolar interaction from molybdenum. However, the very large size of the hyperfine interaction may argue against such a structure.

The structure of the Arsenite signal-giving species is obviously a complex one, with low symmetry around the arsenic, and the simple models presented (Chart I) are evidently not completely adequate. However, a conclusion that can be made with reasonable confidence is that the structure of the signal-giving species is Mo–S–As═, where the two additional bonds from the arsenic are presumably to oxygens. Certainly a Mo–As bond seems to be excluded on the basis of the lack of reaction of arsenite with the desulfo enzyme. In further support of a structure in which the Mo–S bond remains intact is the fact that the arsenite complex of the molybdenum center may be oxidized and reduced in much the same way as can molybdenum of the native enzyme. The analogy should be pointed out between the proposed Mo–S–As═ structure of the arsenite complex on the one hand and the Mo–S–H structure in the Rapid type 1 signal-giving species on the other. In the latter species, the proton, like the arsenic in the former, is strongly coupled to Mo, while the S is relatively weakly coupled (Malthouse et al., 1981; Bray & Gutteridge, 1982). Indeed, a major conclusion from our work is the confirmation it provides of earlier conclusions that there is a molybdenum-bound thiol in the reduced enzyme, which originates from reduction of the terminal sulfur.

The extent to which arsenite blocks the substrate-binding site is of interest. Inhibitors prevent the reaction of arsenite with the enzyme, and substrates such as xanthine do not reduce the arsenite complex. Therefore, the substrate-binding region is obviously modified. On the other hand, substrates and inhibitors do modify the Mo(V) EPR spectrum of the arsenite complex; it is probably significant that small molecules such as salicylate and benzoate have more effect than does xanthine. Presumably the smaller molecules are more capable of entering the substrate-binding region in the presence of arsenite than are the larger ones. Though all these molecules obviously perturb the environment of molybdenum (Figure 1), as shown by the changes in EPR spectral form, we have not attempted simulations. Nevertheless, inspection suggests that relatively small changes in EPR parameters are involved. We therefore suggest that the inhibitors are not liganded directly to molybdenum in the arsenite complex.

Acknowledgments

We are greatly indebted to Dr. R. L. Belford for supplying us with a copy of his EPR simulation program and for advising us on its use. We also thank Teresa Wilkinson for assistance.

Registry No. Molybdenum, 7439-98-7; arsenite, 15502-74-6; xanthine, 69-89-6; benzoic acid, 65-85-0; salicylic acid, 69-72-7; xanthine oxidase, 9002-17-9.

References

Abragam, A., & Bleaney, B. (1970) *Electron Paramagnetic Resonance of Transition Ions*, Clarendon Press, Oxford.

Baratova, Z. R., Semenov, E. V., & Prabhananda, B. S. (1982) *Inorg. Chem. 21*, 57–80.

Barrey, G., Bunbury, G., & Kennaway, E. L. (1928) *Biochem. J. 22*, 1102–1111.

Belford, R. L., & Duan, D. C. (1978) *J. Magn. Reson. 29*, 293–307.

Belford, R. L., & Nilges, M. J. (1979) *Computer Simulation of Powder Spectra, E.P.R. Symposium*, 21st Rockey Mountain Conference, August 1979, Denver, CO.

Bordas, J., Bray, R. C., Garner, D. D., Gutteridge, S., & Hasnain, S. S. (1980) *Biochem. J. 191*, 499–508.

Boyer, P. D., & Bryan, D. M. (1967) *Methods Enzymol. 10*, 60–71.

Bray, R. C. (1975) *Enzymes, 3rd Ed. 12*, 299–419.

Bray, R. C. (1980a) *Adv. Enzymol. Relat. Areas Mol. Biol. 51*, 107–167.

Bray, R. C. (1980b) *Biol. Magn. Reson. 2*, 45–84.

Bray, R. C. (1982) in *Flavins and Flavoproteins* (Massey, V., & Williams, C. H., Eds.) Chapter 130, pp 775–785, Elsevier Biomedical Press, New York.

Bray, R. C., & Gutteridge, S. (1982) *Biochemistry 21*, 5992–5999.

Bray, R. C., Barber, M. J., Lowe, D. J., Fox, R., & Cammack, R. (1975) *FEBS-Symp. 40*, 159–172.

Bray, R. C., Barber, M. J., & Lowe, D. J. (1978) *Biochem. J. 171*, 653–658.

Cammack, R., Barber, M. J., & Bray, R. C. (1976) *Biochem. J. 157*, 469–478.

Cleere, W. L., & Coughlan, M. P. (1974) *Biochem. J. 143*, 331–340.

Coughlan, M. P., Rajagopalan, K. V., & Handler, P. (1969) *J. Biol. Chem. 244*, 2658–2663.

Cramer, S. P., Wahl, R., & Rajagopalan, K. V. (1981) *J. Am. Chem. Soc. 103*, 7721–7727.

Day, E. D., & McClung, R. E. D. (1976) *Inorg. Chem. 15*, 571–577.

Geoffroy, M., & Llinares, A. (1980) *Mol. Phys. 41*, 55–62.

Gutteridge, S., & Bray, R. C. (1980) *Biochem. J. 189*, 615–623.
Gutteridge, S., Tanner, S. J., & Bray, R. C. (1978a) *Biochem. J. 175*, 869–878.
Gutteridge, S., Tanner, S. J., & Bray, R. C. (1978b) *Biochem. J. 175*, 887–897.
Hanson, G. R., Brunette, A. A., McDonell, A. C., Murray, K. S., & Wedd, A. G. (1981) *J. Am. Chem. Soc. 103*, 1953–1959.
Hart, L. I., McGartoll, M. A., Chapman, H. R., & Bray, R. C. (1970) *Biochem. J. 116*, 851–864.
Hille, R., Stewart, R., & Massey, V. (1982) *Fed. Proc., Fed. Am. Soc. Exp. Biol. 41*, 862.
Johnson, J. L., & Rajagopalan, K. V. (1978) *Bioinorg. Chem. 8*, 439–444.
Kubo, M., & Nakamura, D. (1966) *Adv. Inorg. Chem. Radiochem. 8*, 257–282.
Lowe, D. J. (1978) *Biochem. J. 171*, 649–651.
Malthouse, J. P. G., & Bray, R. C. (1980) *Biochem. J. 191*, 265–267.
Malthouse, J. P. G., George, G. N., Lowe, D. J., & Bray, R. C. (1981) *Biochem. J. 199*, 626–637.
Marov, I. N., Dubrov, Yu. N., Belyaeva, V. K., & Ermakov, A. N. (1967) *Dokl. Akad. Nauk SSSR 176*, 530–539; *Dokl. Biochem. (Engl. Transl.) 176*, 835–837.
Massey, V., & Edmondson, D. (1970) *J. Biol. Chem. 245*, 6595–6598.
Maurice, A. M. (1980) Ph.D. Thesis, University of Illinois.
Nilges, M. J. (1979) Ph.D. Thesis, University of Illinois.
Nilges, M. J., & Belford, R. L. (1979) *J. Magn. Reson. 35*, 259–281.
Nilges, M. J., Barefield, E. K., Belford, R. L., & Davies, P. H. (1977) *J. Am. Chem. Soc. 99*, 755–760.
Peters, J. M., & Sanadi, D. R. (1961) *Arch. Biochem. Biophys. 93*, 312–313.
Strickland, S., Palmer, G., & Massey, V. (1975) *J. Biol. Chem. 850*, 4048–4052.
White, L. K., & Belford, R. L. (1976) *J. Am. Chem. Soc. 98*, 4428–4438.

Reactivity of Bovine Blood Coagulation Factor $IX_{a\beta}$, Factor $X_{a\beta}$, and Factor XI_a toward Fluorogenic Peptides Containing the Activation Site Sequences of Bovine Factor IX and Factor X†

Mario J. Castillo, Kotoku Kurachi,‡ Norikazu Nishino, Iwao Ohkubo, and James C. Powers*

ABSTRACT: The published activation site sequences of bovine factors IX and X have been utilized to synthesize a number of peptides specifically designed respectively as substrates for bovine factors XI_a and $IX_{a\beta}$. The substrates contain a fluorophore (2-aminobenzoyl group, Abz) and a quenching group (4-nitrobenzylamide, Nba) that are separated upon enzymatic hydrolysis with a resultant increase in fluorescence that was utilized to measure hydrolysis rates. Factor XI_a cleaved all of the peptides bearing factor IX activation site sequences with Abz-Glu-Phe-Ser-Arg-Val-Val-Gly-Nba having the highest k_{cat}/K_M value. The kinetic behavior of factor XI_a toward the synthetic peptide substrate indicates that it has a minimal extended substrate recognition site at least five residues long spanning S_4 to S_1' and has favorable interactions over seven subsites. The hexapeptide Abz-Glu-Phe-Ser-Arg-Val-Val-Nba was the most specific factor XI_a substrate and was not hydrolyzed by factors $IX_{a\beta}$ or $X_{a\beta}$ or thrombin. Factor $IX_{a\beta}$ failed to hydrolyze any of the synthetic peptides bearing the activation site sequence of factor X. This enzyme slowly cleaved four hexa- and heptapeptide substrates with factor IX activation site sequences extending from P_4 or P_3 to P_3'. Factor $X_{a\beta}$ poorly hydrolyzed all but one of the factor XI_a substrates and failed to cleave any of the factor $IX_{a\beta}$ substrates. Thrombin failed to hydrolyze any of the peptides examined while trypsin, as expected, was highly reactive and not very specific. Phospholipids had no effect on the reactivity of either factors $IX_{a\beta}$ or $X_{a\beta}$ toward synthetic substrates. Both factor $IX_{a\beta}$ and $X_{a\beta}$ cleaved the peptide substrates at similar rates to their natural substrates under comparable conditions. However the rates were substantially lower than optimum activation rates observed in the presence of Ca^{2+}, phospholipids, and protein cofactors. In the future, it may be useful to investigate synthetic substrates that can bind to phospholipid vesicles in the same manner as the natural substrates for factors $IX_{a\beta}$ and $X_{a\beta}$.

The blood coagulation cascade comprises a complex series of biochemical reactions in which inactive zymogens of serine proteases are converted to active blood coagulation enzymes. These enzymes have very high substrate specificities when compared with those of the digestive enzymes such as trypsin. Some stages of the pathway require the formation of discrete complexes between a protease, zymogen, phospholipids, and a protein cofactor. Ca^{2+} ions mediate the interactions among these various species. Factor X, the merging point for both the intrinsic and extrinsic branches of the coagulation pathway, is activated by factor $IX_{a\beta}$.[1] An optimal rate for its activation

† From the School of Chemistry, Georgia Institute of Technology, Atlanta, Georgia 30332 (M.J.C., N.N., and J.C.P.), and the Department of Biochemistry, University of Washington, Seattle, Washington 98195 (K.K. and I.O.). *Received June 23, 1982; revised manuscript received November 5, 1982.* This research was supported by grants to the Georgia Institute of Technology (HL-22530) and to the University of Washington (HL 16919) from the National Institutes of Health.
‡ Recipient of Research Career Development Award HL 00404 from the National Institutes of Health.

[1] The nomenclature for the various coagulation factors is that recommended by an international committee (Wright, 1959). Factor IX_α refers to factor IX with the peptide bond between Arg(146)*Ala(147) cleaved. Factor $IX_{a\alpha}$ refers to factor IX_a with the peptide bond between Arg(181)*Val(182) cleaved. Factor $IX_{a\beta}$ refers to factor IX_a, which does not have activation peptide [Ala(147)–Arg(181)].

0006-2960/83/0422-1021$01.50/0